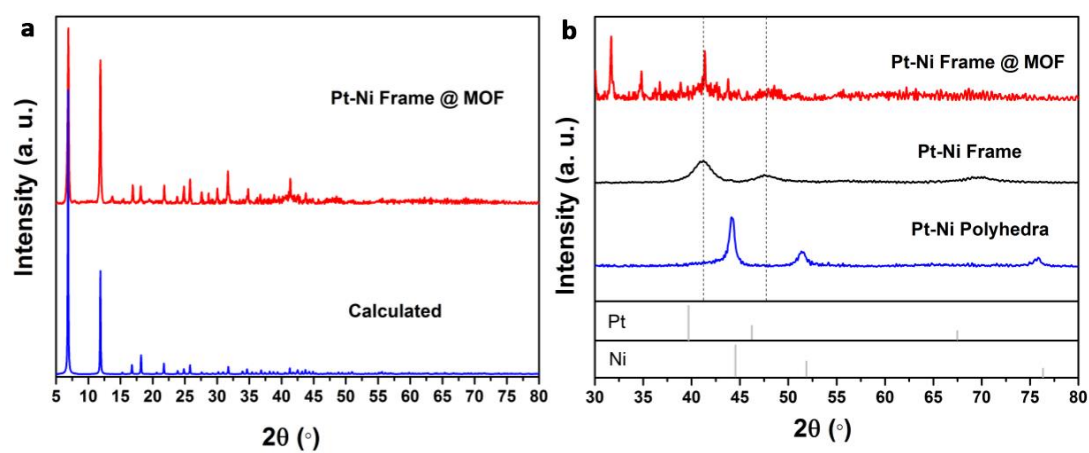
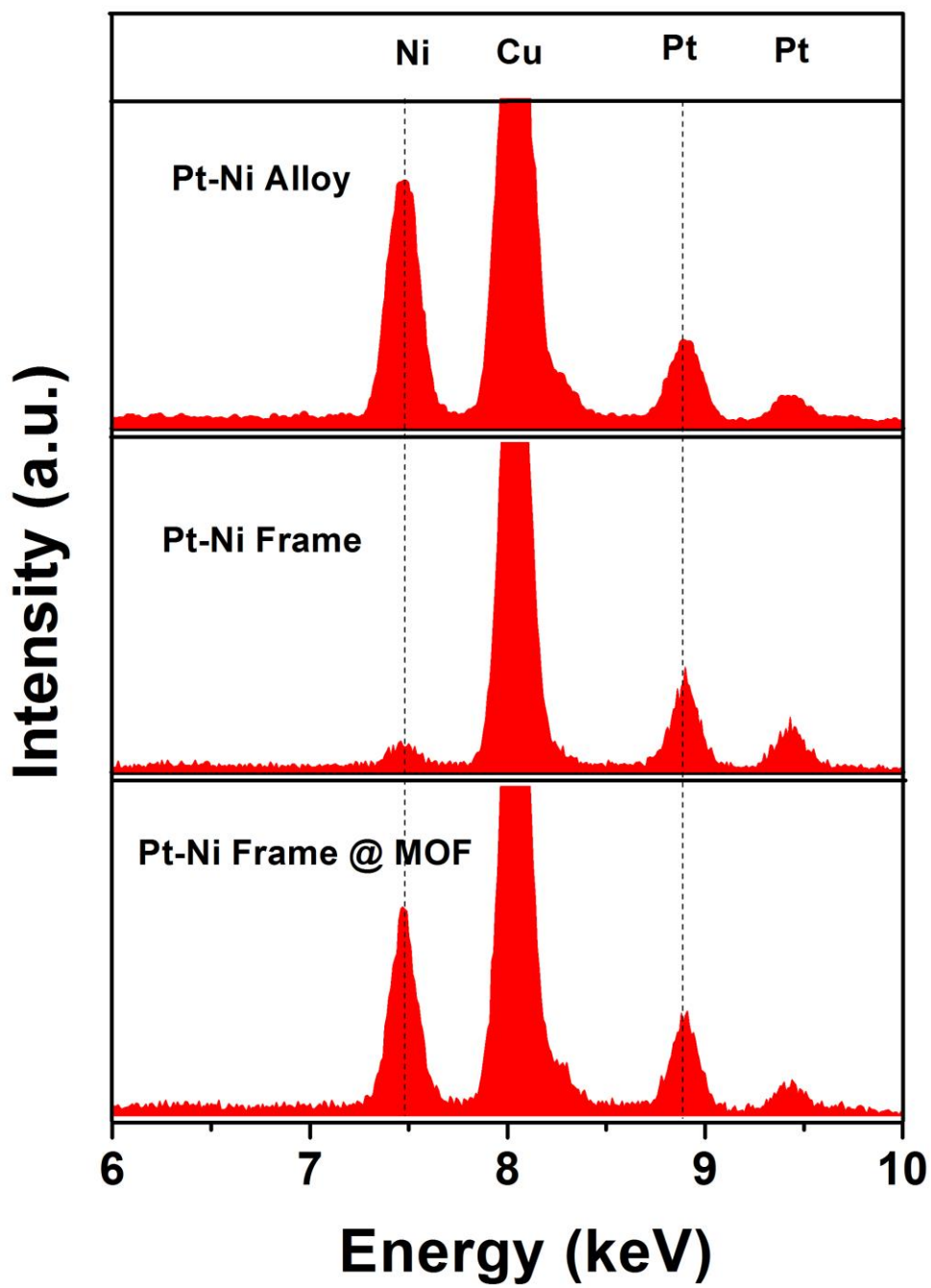


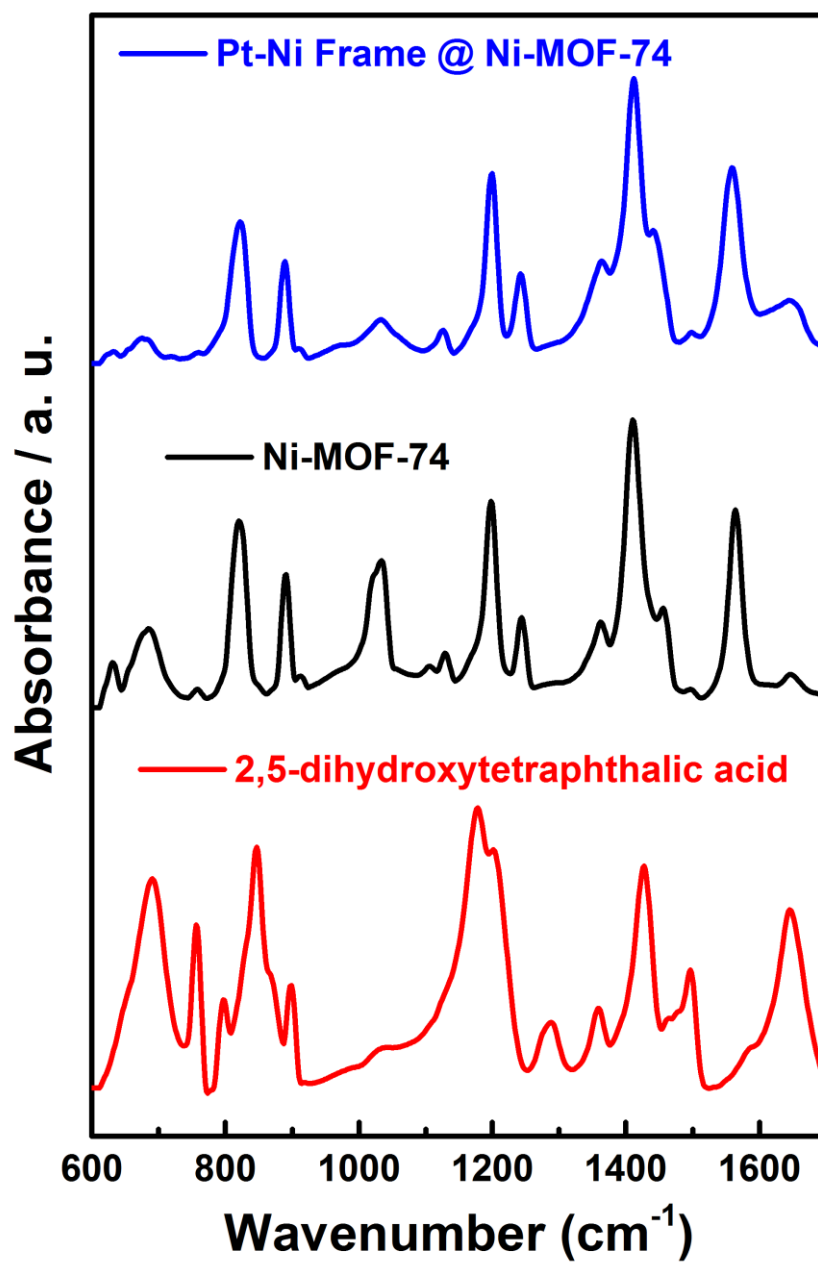
**Supplementary Figure 1.** Low-magnification TEM image of Pt-Ni frame @ MOF. The scale bar is 200 nm.



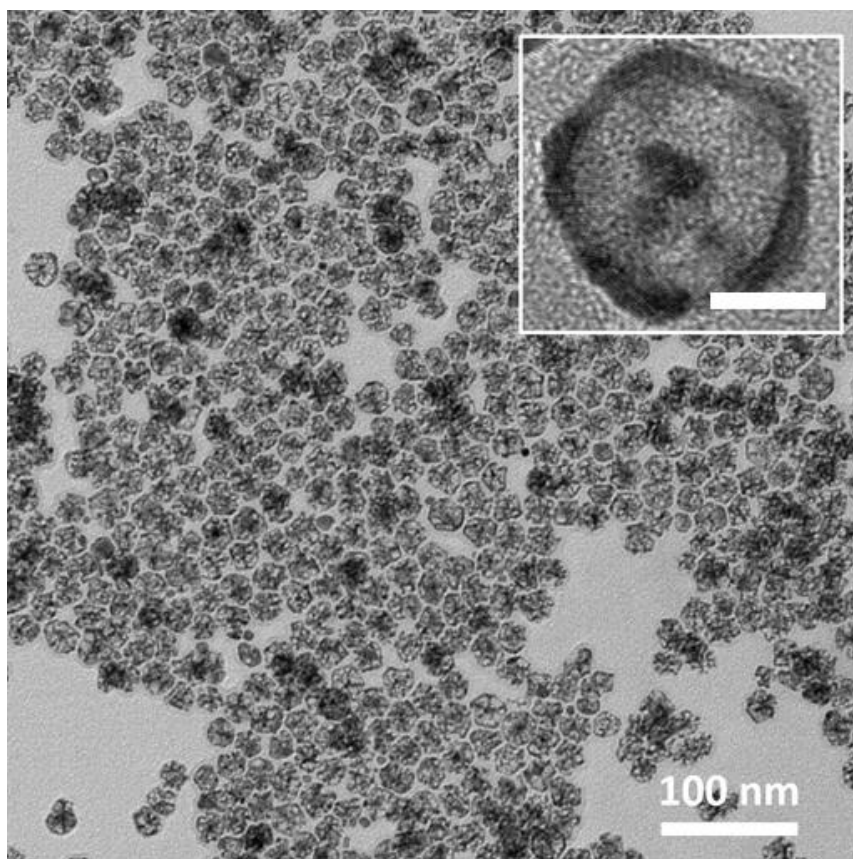
**Supplementary Figure 2.** (a) XRD patterns of the Pt-Ni @ MOF and the simulated Ni-MOF-74 pattern. (b) XRD patterns of Pt-Ni @ MOF, Pt-Ni frames and Pt-Ni polyhedra.



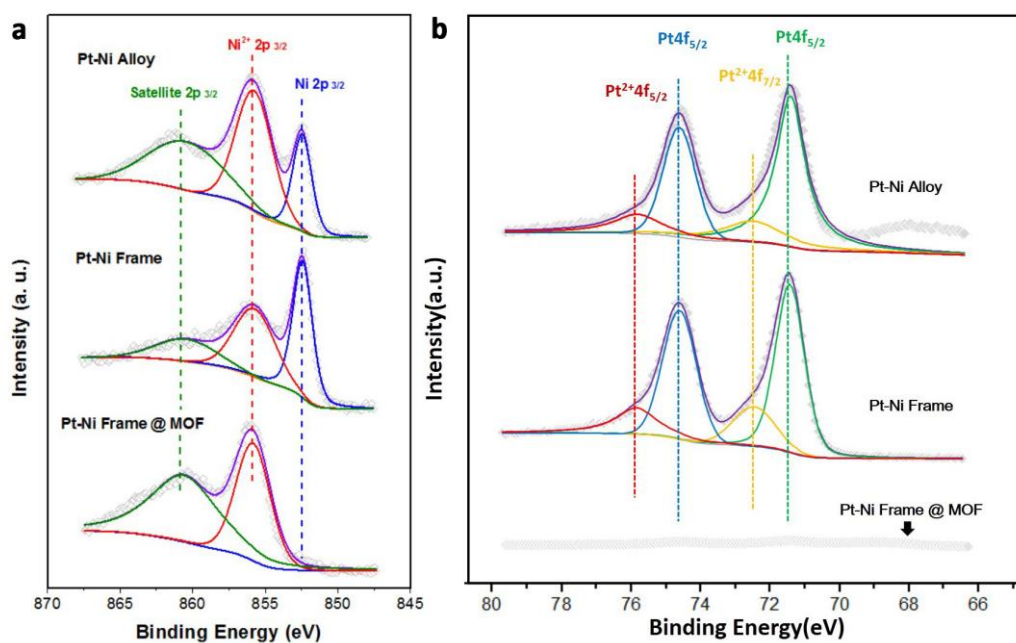
Supplementary Figure 3. EDX spectra of Pt-Ni frame @ MOF, Pt-Ni frame and Pt-Ni polyhedra.



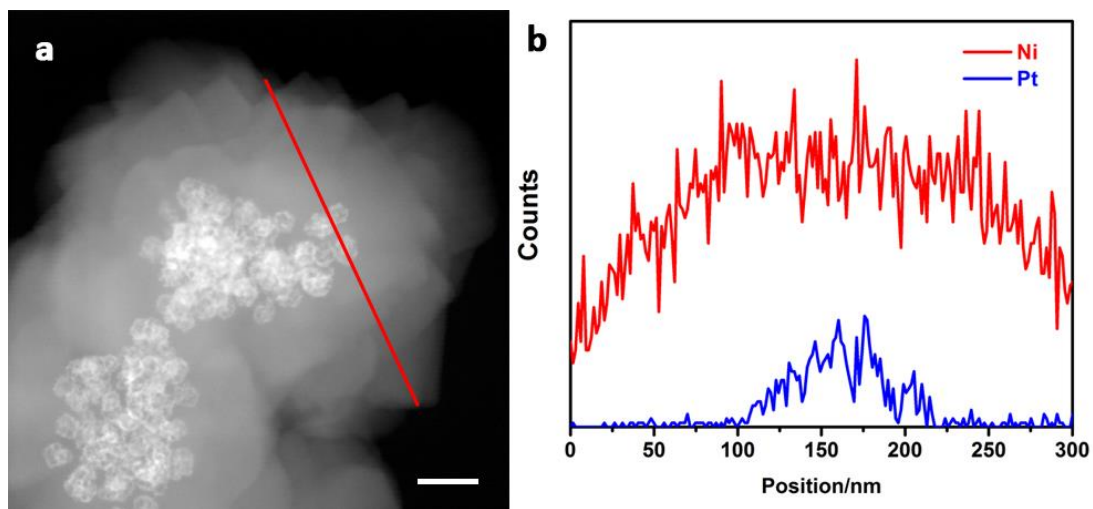
**Supplementary Figure 4.** The fingerprint region of the IR spectra registered for the Pt-Ni frame @ MOF, pure Ni-MOF-74 and the linker 2,5-dihydroxyterephthalic acid. IR spectra of the linker and pure Ni-MOF-74 are remarkably different while there shows a good agreement in band position and relative intensity between Pt-Ni frame @ MOF and pure Ni-MOF-74.



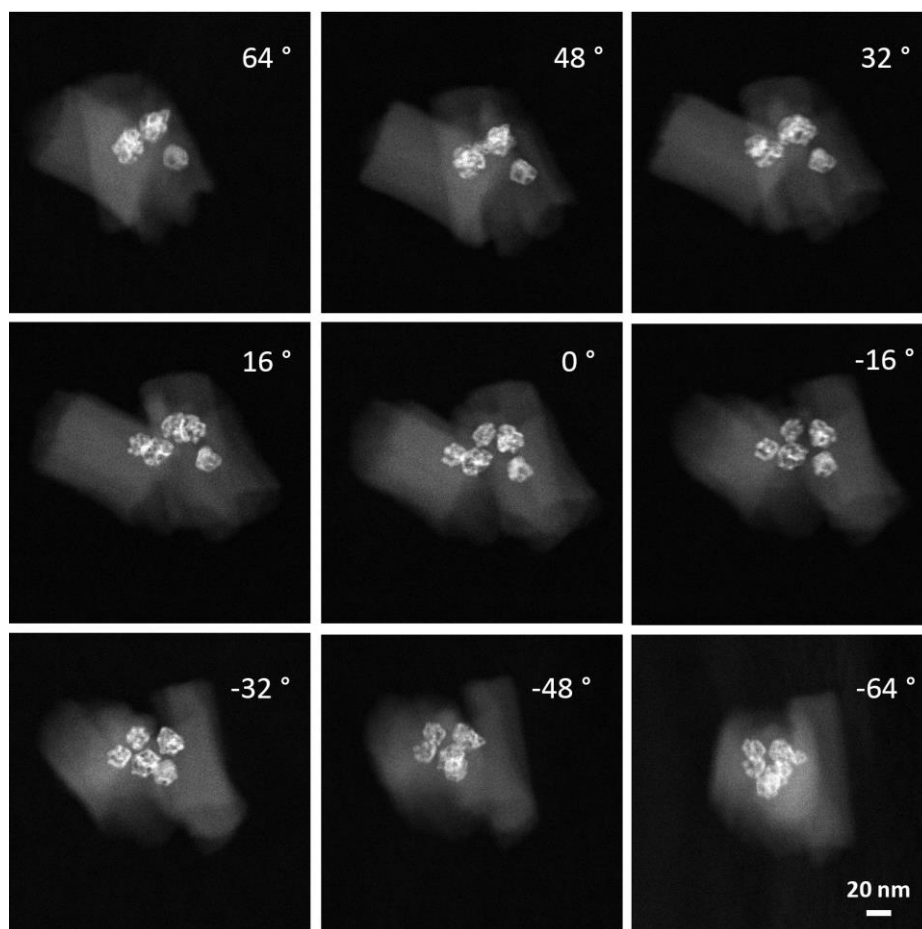
**Supplementary Figure 5.** TEM image of bare Pt-Ni frame and the scale bar is 100 nm. Inset is the magnified TEM image. The scale bar is 10 nm.



**Supplementary Figure 6.** (a) Ni 2p<sub>3/2</sub> and (b) Pt 4f XPS spectra of Pt-Ni polyhedra, Pt-Ni frame, and Pt-Ni frame @ MOF.

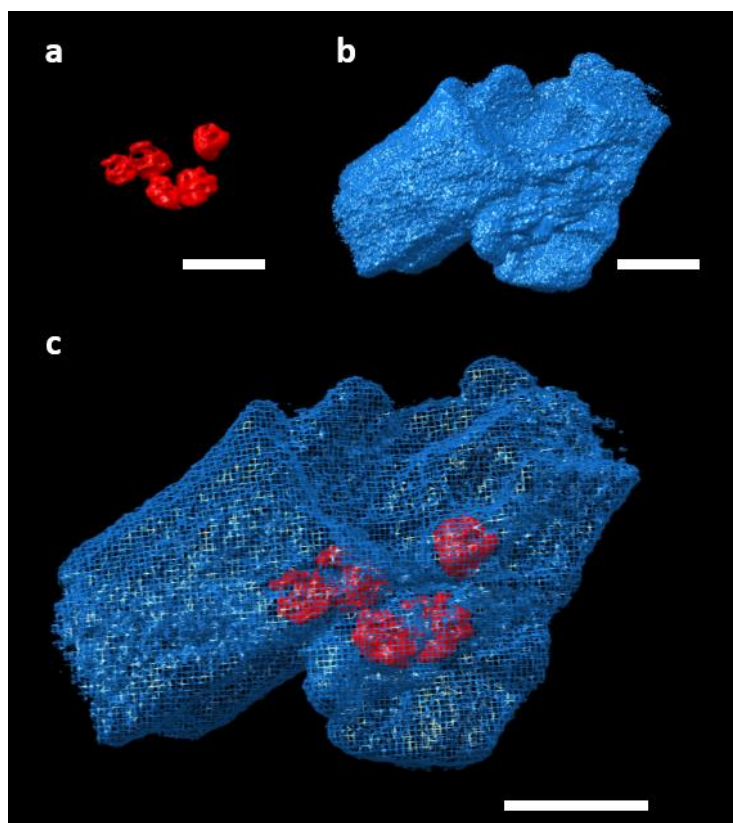


**Supplementary Figure 7.** (a) HAADF-STEM image and (b) cross-sectional compositional line profiles of Pt-Ni frame @ MOF. The scale bar is 10 nm.

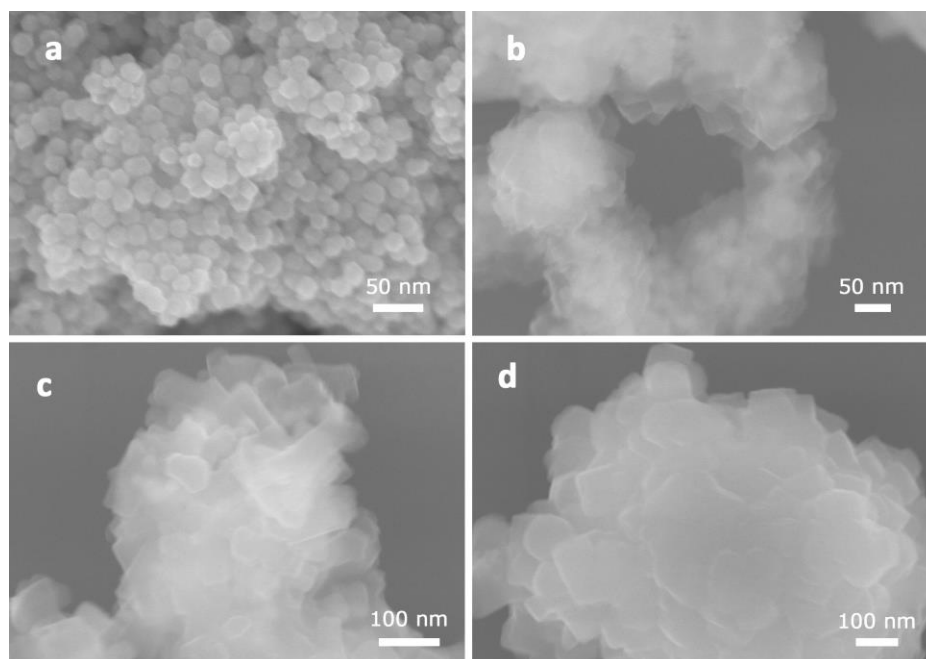


**Supplementary Figure 8.** HAADF STEM images of Pt-Ni frame @ MOF taken at representative tilt angles.

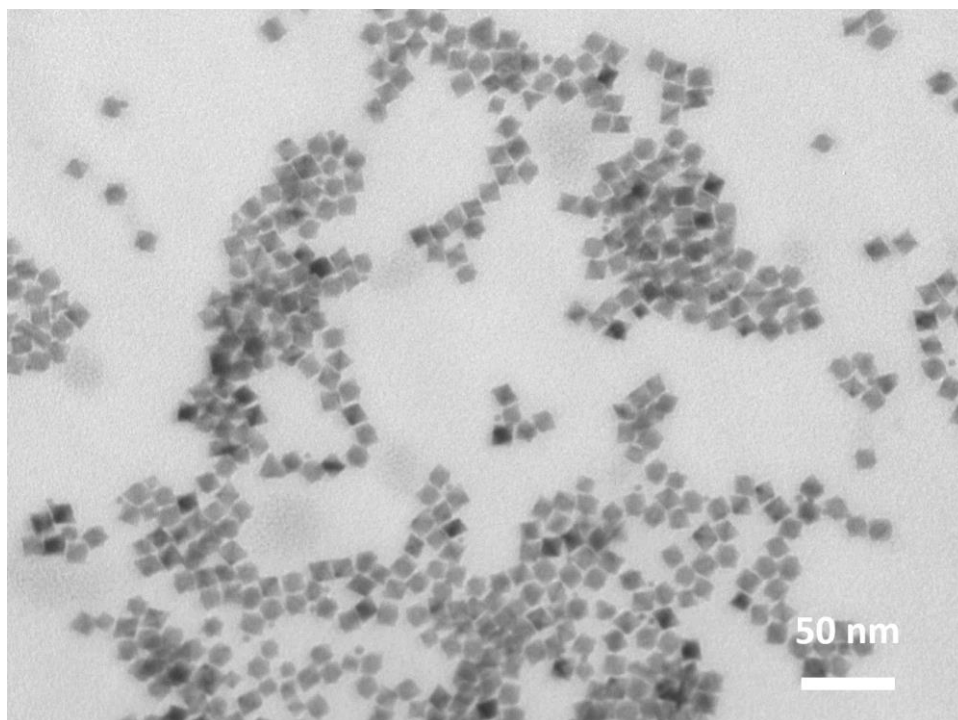




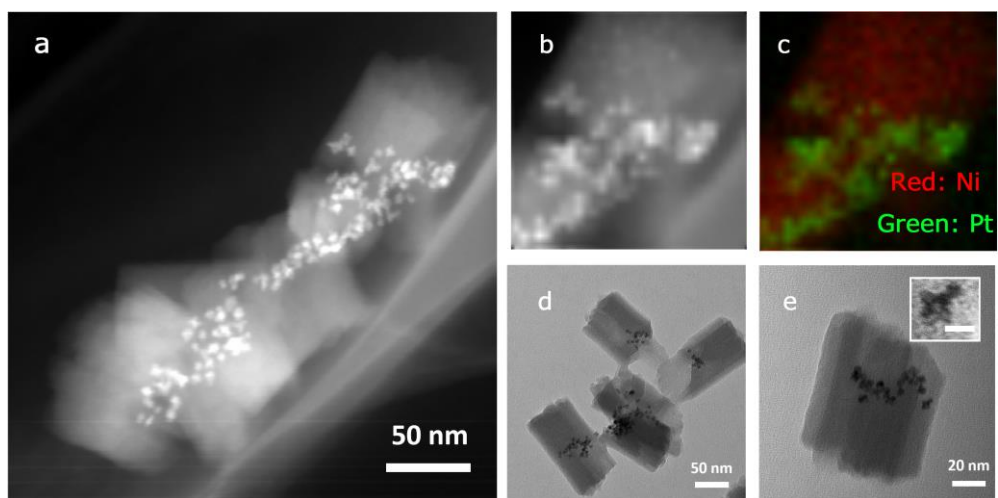
**Supplementary Figure 9.** Tomographic reconstruction of Pt-Ni frame @ MOF. The scale bars are 50 nm.



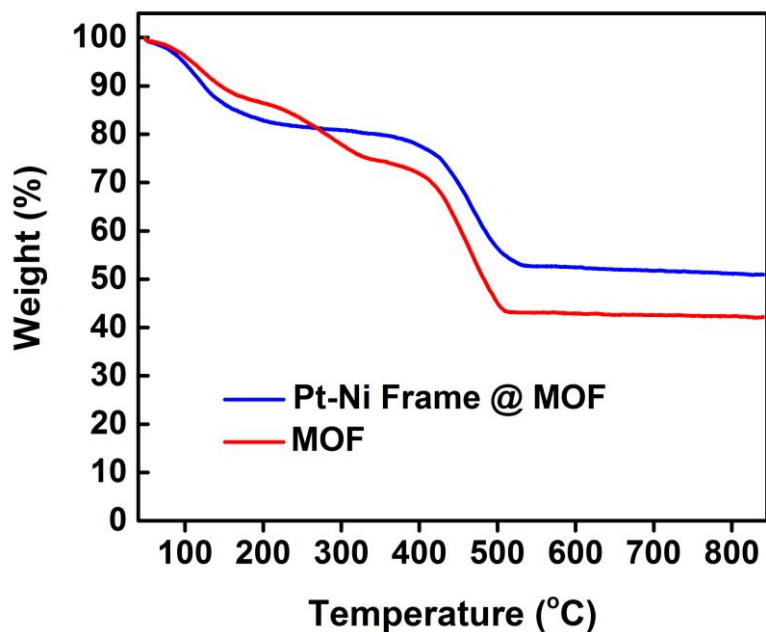
**Supplementary Figure 10.** SEM images showing morphology evolution from Pt-Ni polyhedra to Pt-Ni frame @ MOF sampled at different reaction stages: (a) 0 (b) 2 (c) 4 (d) 12 h.



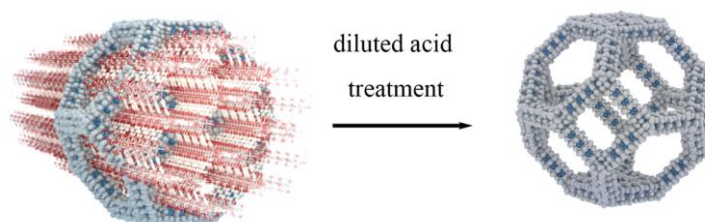
**Supplementary Figure 11.** TEM image of as-obtained octahedral Pt-Ni polyhedra.



**Supplementary Figure 12.** (a), (b) HAADF-STEM image, (c) EDS mapping image and (d), (e) TEM image of concave Pt-Ni alloy @ MOF. Inset is the magnified TEM image showing the concave morphology of Pt-Ni alloy. The scale bar is 5 nm.



**Supplementary Figure 13.** TGA of Pt-Ni Frame @ MOF and Ni-MOF-74. Data were collected under flowing nitrogen using a temperature ramp of  $10^{\circ}\text{C} \cdot \text{min}^{-1}$ .

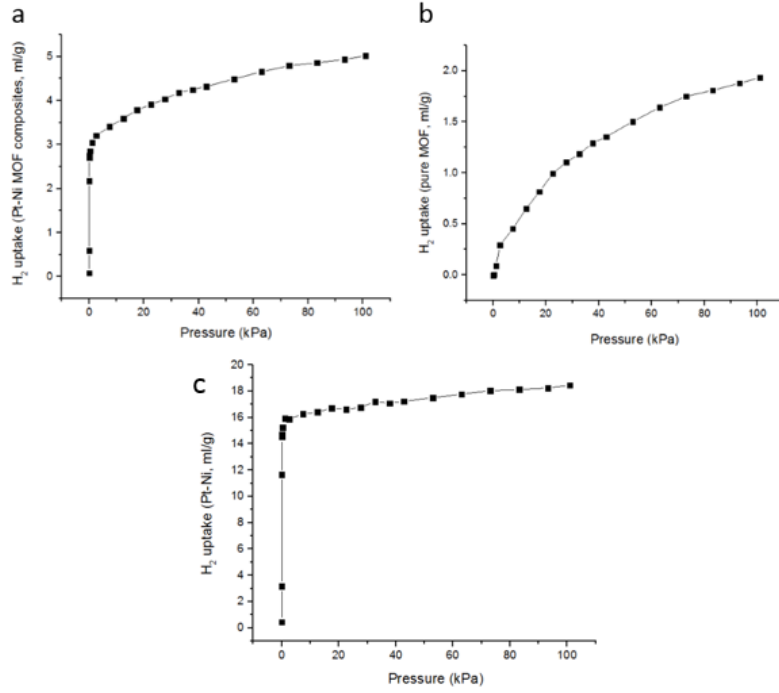


**Supplementary Figure 14.** Scheme showing the structural transformation from Pt-Ni frame @ MOF to bare Pt-Ni frame by acid treatment. From ICP-MS measurement, the Pt:Ni molar ratios within Pt-Ni frame @ MOF and bare Pt-Ni nanoframe are 1:6.7 and 1:0.5, respectively. Hence, the molar ratio of Pt : Ni (in nanoframe) : Ni(in MOF) is 1 : 0.5 : 6.2. As the stoichiometric ratio of Ni : ligand in Ni-MOF-74 is 2:1, the molecular formula of Pt-Ni frame @ MOF should be  $\text{PtNi}_{0.5}(\text{Ni}_2\text{L})_{3.1}$  and the mass fractions of Pt-Ni frame (core) and MOF (shell) could be obtained according to equation (1) and (2).

$$\omega_{\text{PtNi}} = \frac{(195.1+58.7*0.5)}{(195.1+58.7*0.5)+(58.7*2+198.1)*3.1} = 0.19 \quad (1)$$

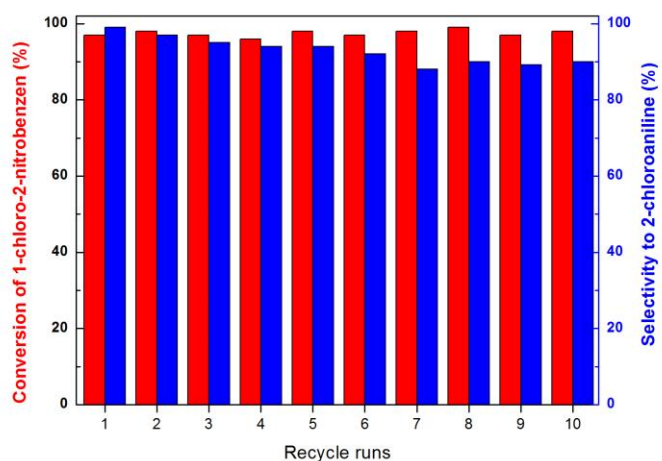
$$\omega_{\text{MOF}} = \frac{(58.7*2+198.1)*3.1}{(195.1+58.7*0.5)+(58.7*2+198.1)*3.1} = 0.81 \quad (2)$$



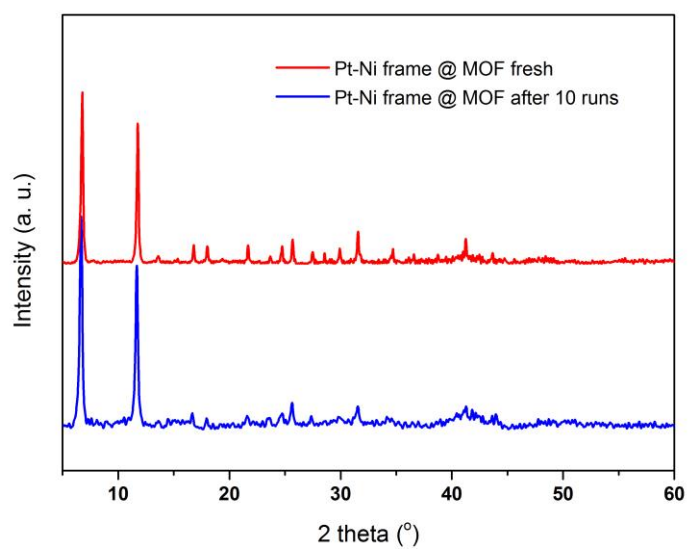


**Supplementary Figure 15.** Hydrogen adsorption capacity of (a) Pt-Ni frame @ MOF and (b) pure MOF. Calculated hydrogen adsorption capacity (c) of Pt-Ni frame in the Pt-Ni frame @ MOF. For the Pt-Ni frame @ MOF composites ( $C_{\text{PtNi core-MOF}}$ ), the uptake capacity of H<sub>2</sub> were suggested to contain two parts:  $C_{\text{PtNi core}}$  ( $\text{mL}\cdot\text{g}^{-1}$ ) for the encapsulated Pt-Ni alloy core and  $C_{\text{MOF}}$  ( $\text{mL}\cdot\text{g}^{-1}$ ) for MOF. The total uptake  $C_{\text{PtNi core-MOF}}$  ( $\text{mL}\cdot\text{g}^{-1}$ ) was considered to be the weighted arithmetic mean of  $C_{\text{PtNi core}}$  and  $C_{\text{MOF}}$ . Hence, the calculated  $C_{\text{PtNi core}}$  can be obtained by equation (3).

$$C_{\text{PtNi core}} = (C_{\text{PtNi core-MOF}} - C_{\text{MOF}} \cdot \omega_{\text{MOF}}) / \omega_{\text{PtNi core}} \quad (3)$$

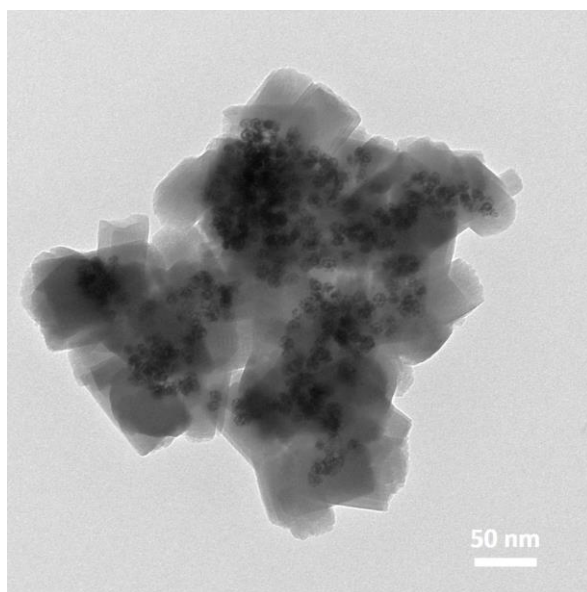


**Supplementary Figure 16.** The recycle experiment of selective hydrogenation of 1-chloro-2-nitrobenzene. Reaction conditions: 1-chloro-2-nitrobenzene (0.3 mmol), [Pt] (1mg, 1.6 mol%), CH<sub>3</sub>OH (1.5 mL), PH<sub>2</sub>: 1 bar, T: 30 °C, 90min.

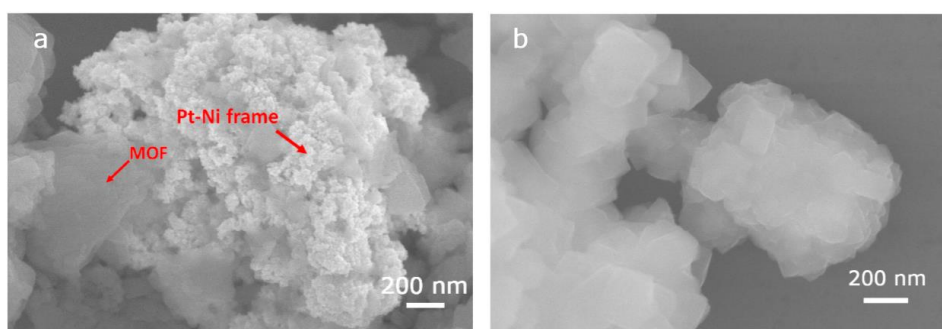


h

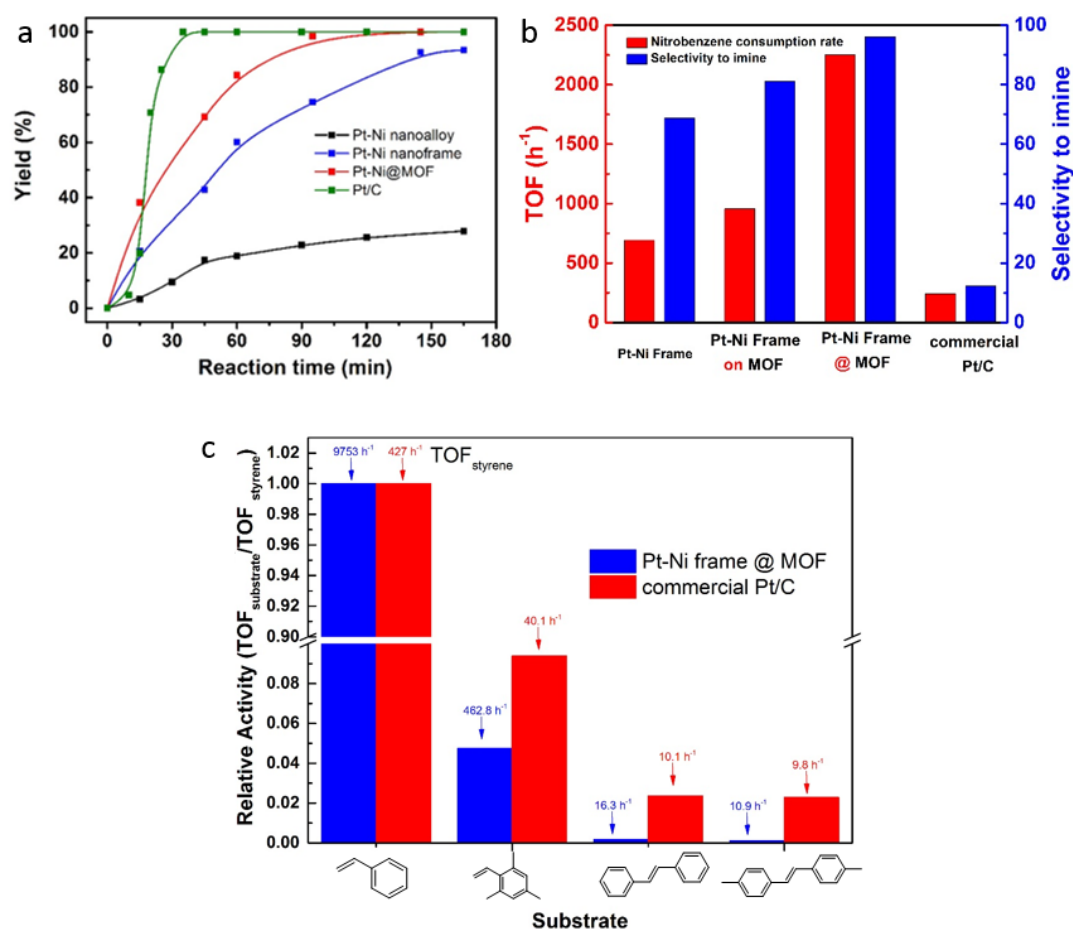
**Supplementary Figure 17.** PXRD of Pt-Ni frame @ MOF after 10 catalytic runs.



**Supplementary Figure 18.** TEM image of Pt-Ni frame @ MOF after 10 catalytic runs.



**Supplementary Figure 19.** SEM images of (a) the Pt-Ni frame on MOF and (b) Pt-Ni frame @ MOF catalysts, showing the different topological structure.



**Supplementary Figure 20.** The catalytic activity of commercial Pt/C compared with Pt-Ni alloy and Pt-Ni frame @ MOF in the hydrogenation of 1-chloro-2-nitrobenzene, reductive imination of nitrobenzene, and hydrogenation of olefins. (a) 1-chloro-2-nitrobenzene (0.3 mmol), catalysts [Pt] (0.005 mmol), CH<sub>3</sub>OH (1.5 mL), PH<sub>2</sub>: 1 bar, T: 30 °C. (b) nitrobenzene (0.2 mmol), benzaldehyde (0.3 mmol), catalysts containing [Pt] (0.005 mmol), C<sub>2</sub>H<sub>5</sub>OH (2 mL), PH<sub>2</sub>: 1 bar, T: 30 °C. The TOF values were calculated based on the active sites measured from the CO titration experiments. (c) olefins (styrene, 2,4,6-trimethylstyrene, trans-stilbene, 4,4'-dimethyl-trans-stilbene) (0.1 mmol for each component), catalysts containing [Pt] (0.0025 mmol), THF (1.5 mL), PH<sub>2</sub>: 1 bar, T: 30 °C.

**Supplementary Table 1.** Composition of Pt-Ni nanostructures

Entry	Analyzed molar ratios	Analyzed molar ratios
	(Pt-Ni) by ICP-MS	(Pt-Ni) by EDS
Pt-Ni Polyhedra	0.11 0.89	0.13 0.87
Pt-Ni Frame	0.68 0.32	0.71 0.29
Pt-Ni Frame @ MOF	0.13 0.87	0.16 0.84

**Supplementary Table 2.** Catalytic activity comparison among Ni based materials and Pt-Ni frame @

MOF

Entry	Conv. (%)
Pt-Ni frame@Ni-MOF-74 <sup>a</sup>	>99.0
Ni nanocrystal <sup>a</sup>	N.D.
Ni-MOF-74 <sup>a</sup>	N.D.
Pt-Ni frame@Ni-MOF-74 <sup>b</sup>	>99.0
Ni nanocrystal <sup>b</sup>	N.D.
Ni-MOF-74 <sup>b</sup>	N.D.
Pt-Ni frame@Ni-MOF-74 <sup>c</sup>	>99.0
Ni nanocrystal <sup>c</sup>	N.D.
Ni-MOF-74 <sup>c</sup>	N.D.

<sup>a</sup> 1-chloro-2-nitrobenzene (0.3 mmol), [Ni] (10 mol%), CH<sub>3</sub>OH (1.5 mL), PH<sub>2</sub>: 1 bar, T: 30 °C, 3 h.

<sup>b</sup> styrene (0.1 mmol), [Ni] (10 mol%), THF (1.5 mL), PH<sub>2</sub>: 1 bar, T: 30 °C, 3 h.

<sup>c</sup> nitrobenzene (0.2 mmol), benzaldehyde (0.3 mmol), [Ni] (10 mol%), C<sub>2</sub>H<sub>5</sub>OH (2 mL), PH<sub>2</sub>: 1 bar, T: 30 °C, 3 h.



**Supplementary Table 3.** CO chemisorption measurements at 323K

CO chemisorption measurements at 323K

Entry	Sample	Metal(0) content ( wt. % )	CO chemisorption ( $\mu\text{mol/g catalyst}$ )	active sites per gram metal * ( $\mu\text{mol/g metal}$ )	Dispersion ** ( $\text{mol}_{\text{active sites}}/\text{mol}_{\text{metal, \%}}$ )
1	Pt-Ni frame	100	256.4	256.4	3.8
2	Ni-MOF-74	0	4.5	-	-
3	Pt-Ni frame @ MOF	19	35.5	159.5	2.4
4	Pt-Ni frame on MOF	19	45.5	209.5	3.1
5	Pt/C***	5	189.7	3794	73.8

The active site number and dispersion were calculated assuming a stoichiometry of one CO molecule per surface metal atom (metal atom = Pt + Ni).

\*From entry 1 and 2, it is showed that the CO chemisorption on Ni-MOF-74 is significantly lower than Pt-Ni frame core. In this column we deducted the chemisorption of Ni-MOF-74 part and normalize the CO uptake amount based on the total metal weight (Pt + Ni) of Pt-Ni nanostructures and Pt/C. We assume a stoichiometry of one CO molecule per surface active site to calculate the active sites per gram metal.

\*\*As it is hard to exclude the catalytic role of Ni metal due to the possible synergetic interaction between Pt and Ni atoms, we calculate the dispersion of Pt-Ni nanostructures base on the total metal number (Pt + Ni).

\*\*\*It has been inferred that carbon materials did not show CO chemisorption capability<sup>2</sup>.

### Supplementary References

- 1 Li, G. *et al.* Hydrogen storage in Pd nanocrystals covered with a metal–organic framework. *Nature Mater.* **2014**, *13*, 802–806.
- 2 Kirilin, A. V. *et al.* Aqueous-phase reforming of xylitol over Pt/C and Pt/TiC-CDC catalysts: catalyst characterization and catalytic performance. *Catal. Sci. Technol.* **2014**, 387–401.